

# The Formation and Growth of Intermetallic Compounds in Sn-Zn and Sn-Zn-Al Solder with Ni/Au Surface Finish Bond Pad

SHIH-CHANG CHANG,<sup>1</sup> SHENG-CHIH LIN,<sup>1</sup> and KER-CHANG HSIEH<sup>1,2</sup>

1.—Institute of Materials Science and Engineering, Center for Nanoscience and Nanotechnology, National Sun Yat-Sen University, Kaohsiung, Taiwan 804, Republic of China. 2.—E-mail: khsieh@mail.nsysu.edu.tw

In this study, we used microstructure evolution and electron microprobe analysis (EPMA) to investigate the interfacial reactions in Sn-Zn and Sn-Zn-Al solder balls with Au/Ni surface finish ball-grid-array (BGA) bond pad over a period of isothermal aging at 150°C. During reflow, Au dissolved into the solder balls and reacted with Zn to form  $\gamma$ -Au<sub>3</sub>Zn<sub>7</sub> and  $\gamma_2$ -AuZn<sub>3</sub>. As aging progressed,  $\gamma$  and  $\gamma_2$  transformed into  $\gamma_3$ -AuZn<sub>4</sub>. Finally, Zn precipitated out next to  $\gamma_3$ -AuZn<sub>4</sub>. The Zn reacted with the Ni layer to form Ni<sub>5</sub>Zn<sub>21</sub>. A thin layer (Al, Au, Zn) intermetallic compound (IMC) formed at the interface of the Sn-Zn-Al solder balls, inhibiting the reaction of Ni with Zn. Even after 50 days of aging, no Ni<sub>5</sub>Zn<sub>21</sub> was observed. Instead, fine (Al, Au, Zn) particles similar to Al<sub>2</sub> (Au, Zn) in composition formed and remained stable in the solder. The lower ball shear strength corresponded with the brittle fracture morphology in Sn-Zn-Al solder ball samples.

**Key words:** Sn-Zn solder, Sn-Zn-Al solder, Au-Zn intermetallic compound, Ni-Zn intermetallic compound, reliability

## INTRODUCTION

In the manufacture of products with many micro-electronic devices, ball-grid-array (BGA) has been used for packaging, because it is smaller and performs better than traditional devices. However, the lead in Sn-Pb solders, which are often used in BGAs, may be harmful to the environment and human health. To avoid this hazard, Sn-Ag- and Sn-Zn-based solders might possibly serve as lead-free substitutes for Sn-Pb solders.

The Au/Ni surface finish is a commonly used metallization in the bond-pad structure of the BGA package. The Au layer provides protection from oxidation, and the Ni layer serves as a diffusion layer that inhibits the reaction between the solder and the Cu layer. The interfacial reaction of solders with substrates may affect reliability.<sup>1</sup> As many studies on the reaction of Sn-Ag-Cu solders with various substrates have shown,<sup>2–5</sup> the brittle nature of the intermetallic compound (IMC), the growth of IMC,

and the formation of voids cause significant degradation. Kim et al.<sup>6,7</sup> investigated the behavior of Sn-Zn solder balls on the Au/Ni/Cu pad and found that  $\beta$ -AuZn and three divided  $\gamma$ -Ni<sub>5</sub>Zn<sub>21</sub> layers at the interface. Date et al.<sup>8,9</sup> have reported the reaction products of Sn-Zn solder balls at the interface to be thin layers of  $\epsilon$ -AuZn<sub>8</sub>.

Aluminum has been added to Sn-Zn solder balls to reduce oxidation. The Al of the solder balls tends to aggregate at the interface and form an IMC, which acts as an inherent barrier inhibiting the reaction of solder balls and substrates.<sup>10–15</sup> In this study, we used microstructure evolution and electron microprobe analysis (EPMA) to investigate the interfacial reactions of Sn-Zn and Sn-Zn-Al solder balls with Au/Ni surface finishes over a period of isothermal aging at 150°C.

## EXPERIMENTAL PROCEDURE

Specimens for this study were solder balls made of eutectic Sn-9Zn and Sn-7.23Zn-0.01Al solders. The ball size was 760  $\mu\text{m}$  in diameter. The under bump metallization (UBM) of BGA256 bond pads had an

Au/Ni/Cu layer. The surface finish was created by electrolytic Ni/Au plating. The Au layer had a thickness of 0.5–0.7  $\mu\text{m}$ , and the Ni layer 6–8  $\mu\text{m}$ . The infrared reflow temperature profile was done by holding at 150°C for 2 min., heating to 230°C, and then cooling. The samples were aged in a convection oven set at 150°C for up to 50 days. The specimens were cross sectioned after certain aging periods, mounted in a room-temperature curing epoxy, and polished using 3- $\mu\text{m}$  and 1- $\mu\text{m}$  diamond paste. The composi-

tions of phases in the solder balls and the interface were quantitatively measured with an EPMA.

### RESULTS AND DISCUSSION

#### Reaction of Sn-9Zn Solder Balls with the Au/Ni Surface Finish

Figure 1 shows the cross-sectional micrographs of Sn-9Zn solder balls at 150°C isothermal aging. The Sn-9Zn solder balls consisted of  $\beta\text{-Sn}$  (the matrix

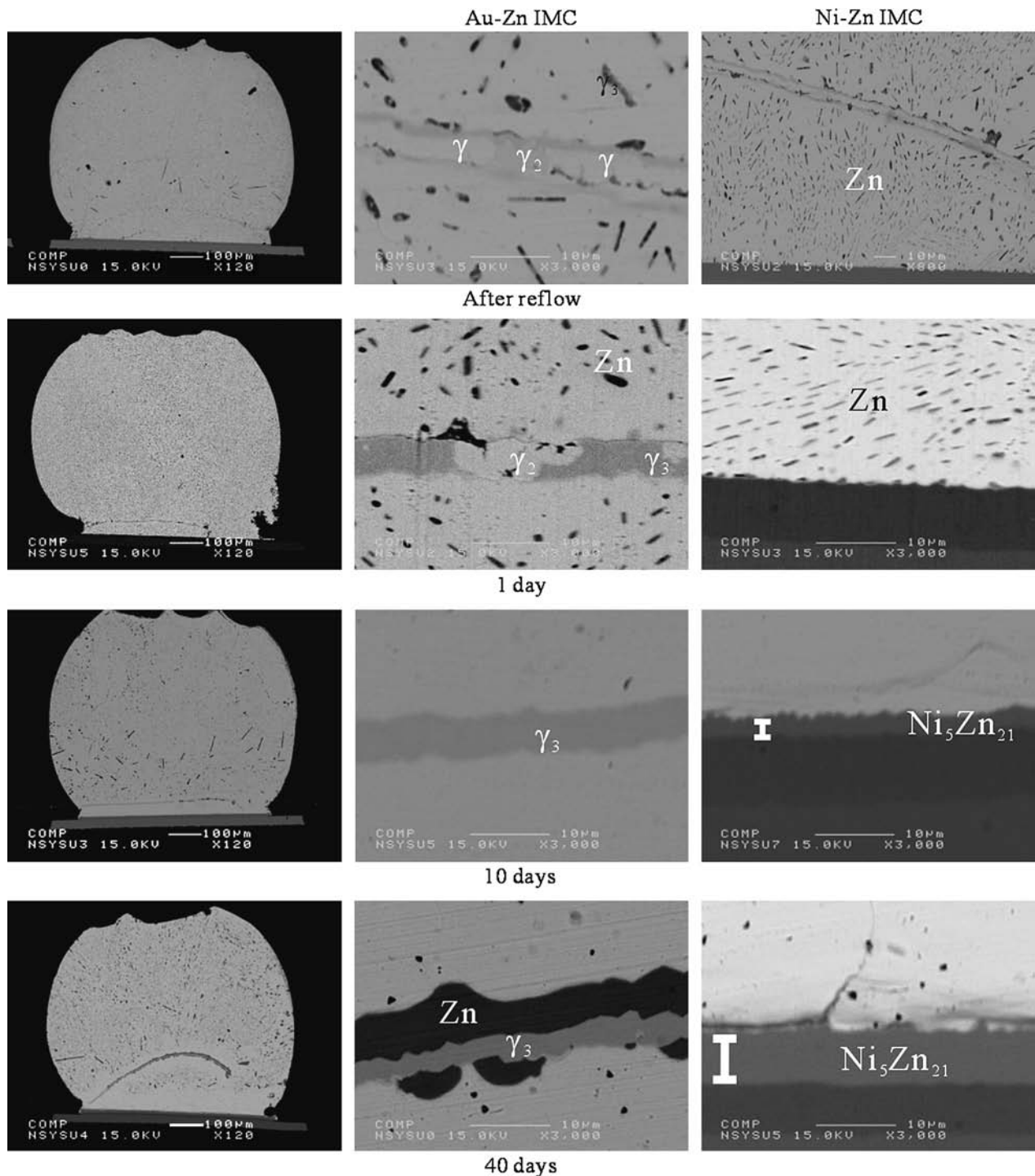
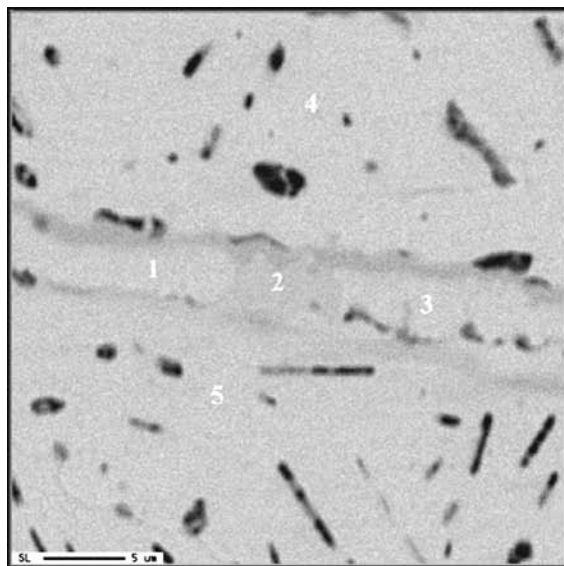


Fig. 1. SEM micrographs of Sn-9Zn solder balls with 150°C aging in various days.

phase seen as bright gray) and Zn (the dispersed phase seen as dark gray). After reflow, bands were observed in the bottom side of the balls. The Au layer over the Ni layer dissolved into liquid solder and formed the band-shaped IMC above the interface. Over the aging period, we were able to observe changes of IMC in the interface and the band-shaped IMC inside the solder ball. The band-shaped IMC was confirmed to be composed of various Au-Zn IMCs including a very limited amount of Sn.

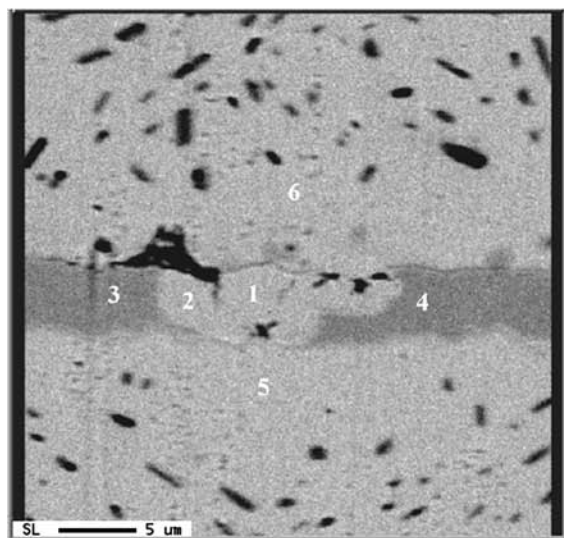
Figure 2 shows the results of the microprobe analysis of the band-shaped IMC. After reflow, the band-shaped IMC was confirmed by EPMA to be  $\gamma$ -Au<sub>3</sub>Zn<sub>7</sub> and  $\gamma_2$ -AuZn<sub>3</sub> composed of 70–74% Au and 25–29% Zn, according to the Au-Zn binary phase diagram.<sup>16</sup> Both reflow phases in our study were different from those reported by Kim et al., whose transmission electron microscopy–energy-dispersive spectroscopy

analysis found  $\beta$ -AuZn to be composed of 47.4at.%Au and 52.6at.%Zn.<sup>6,7</sup> This difference may have resulted from a difference in the setup of reflow temperature profile. In our study, the plated Au layer dissolved and diluted into liquid solder more homogeneously than it did in Kim's samples. In our study,  $\gamma$ -Au<sub>3</sub>Zn<sub>7</sub> and  $\gamma_2$ -AuZn<sub>3</sub> formed from liquid solder instead of  $\beta$ -AuZn with higher Au content in Kim's study. After 1 day of aging, the Au-Zn IMC gradually changed from  $\gamma_2$ -AuZn<sub>3</sub> to  $\gamma_3$ -AuZn<sub>4</sub>, consisting of 80–84% Au and 18–19% Zn. These two phases had clearly different lightness of gray, so they were easily identified. After 10 days of aging, the band-shaped phase had completely converted into  $\gamma_3$ -AuZn<sub>4</sub>. After 40 days, the Zn phase had precipitated near the band-shaped phase. We clearly observed a dark Zn phase near  $\gamma_3$ -AuZn<sub>4</sub> (Fig. 3a). This  $\gamma_3$ -AuZn<sub>4</sub> phase was different from the  $\epsilon$ -AuZn<sub>8</sub> phase reported by Date et al.<sup>8,9</sup> The present aging condition may not



a

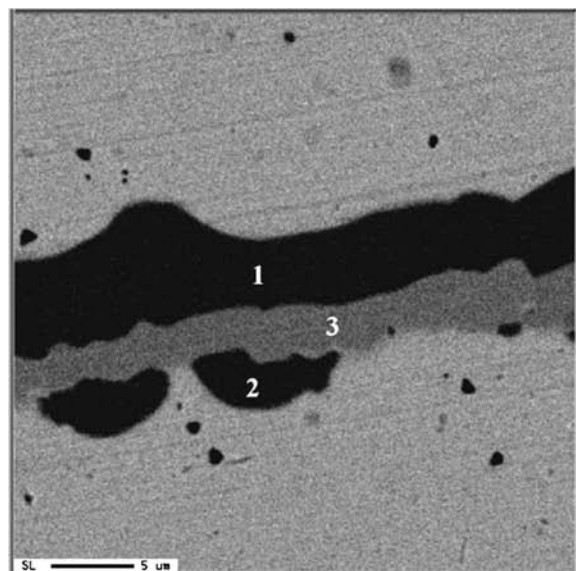
Atomic ratio					
No.	Sn	Zn	Ni	Au	Comment
1	0.4	70.02	0.08	29.5	$\gamma$
2	0.36	74.64	0.03	24.98	$\gamma_2$
3	0.95	70.02	0.15	28.88	$\gamma$
4	97.29	2.18	0	0.53	
5	97.66	1.78	0.02	0.55	



b

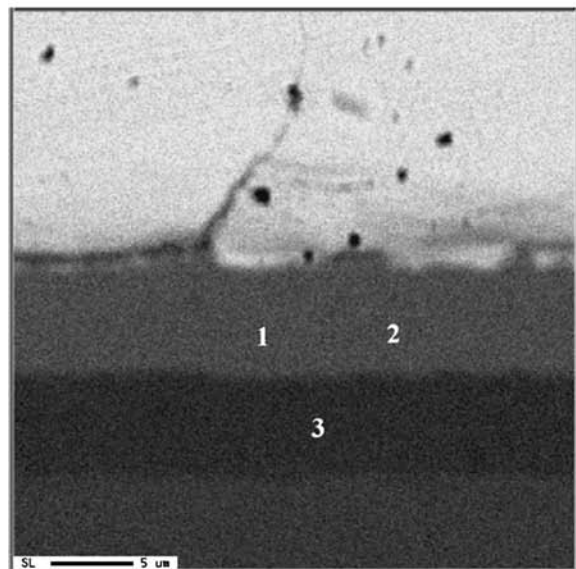
Atomic ratio					
No.	Sn	Zn	Ni	Au	Comment
1	0.27	72.16	0.05	27.52	$\gamma_2$
2	0.38	72.45	0.04	27.13	$\gamma_2$
3	0.29	81.54	0	18.17	$\gamma_3$
4	0.23	81.02	0.04	18.71	$\gamma_3$
5	97.35	2.14	0	0.52	
6	96.54	2.85	0.01	0.61	

Fig. 2. Quantitative analysis of the Au-Zn IMC in Sn-9Zn solder balls: (a) as reflow and (b) 1 day aging.



Atomic ratio					
No.	Sn	Zn	Ni	Au	comment
1	0.47	96.2	0.02	3.33	Zn
2	0.23	97	0	2.77	Zn
3	0.2	81.14	0.11	18.54	$\gamma_3$

a



Atomic ratio					
No.	Sn	Zn	Ni	Au	comment
1	0.14	80.23	19.12	0.23	$Ni_5Zn_{21}$
2	0.17	81.03	18.75	0.05	$Ni_5Zn_{21}$
3	0.04	0.52	99.21	0.21	

b

Fig. 3. Quantitative analysis of the Au-Zn IMC in Sn-9Zn solder balls: (a) band-shaped phase region after 40 days of aging and (b) interface region after 40 days of aging.

have reached the final thermodynamic equilibrium, according to the Au-Zn binary phase diagram.

Because Au dissolved into the solder, the Ni layer came into direct contact with the Sn-9Zn solder, and, with aging, formed IMC. The Ni-Zn IMC was confirmed quantitatively as  $Ni_5Zn_{21}$  (Fig. 3b), as depicted in the Ni-Zn phase diagram.<sup>17</sup> These results were the same as those reported by Chan et al.<sup>18</sup> and Kim et al.<sup>5-6</sup>  $Ni_5Zn_{21}$  grew gradually over time to a thickness of 2  $\mu\text{m}$  after 5 days of aging. After 50 days, IMC had in some cases grown to a thickness of 8  $\mu\text{m}$ . The Ni layer on the Cu pad is used to prevent Cu from reacting with the solder. In this testing condition, the Ni layer seemed to work well and Cu maintained its original status.

With regard to the Au-Zn IMC, Au quickly dissolved into the solder after reflow and formed the band-shaped phase. Because Au was consumed during the reflow, there was no change in size of this Au-Zn IMC, even after 50 days of aging. Although Sn often reacts with other components in the Sn-Pb and Sn-Ag-Cu solders,<sup>2-5</sup> its solubility in these IMC was limited in the Sn-Zn-X type solder. The Zn continually diffused into the Au-Zn IMC and the Ni-Zn IMC. There was a Zn-free zone in which spots corresponding to Zn-rich phases disappeared in peripheral regions of the band and the interface. We observed a gradual expansion of the Sn-phase zone without the Zn phase to the bottom side of the solder balls within 40 days of aging (Fig. 1).

### Reaction of Sn-Zn-Al Solder Balls with the Au/Ni Surface Finish

The Au layer dissolved into the solder ball during reflow (Fig. 4), forming the band-shaped phase, the same reaction as was seen in the Sn-9Zn solder balls. This band-shaped phase was confirmed as  $\gamma$ -Au<sub>3</sub>Zn<sub>7</sub> and  $\gamma_2$ -AuZn<sub>3</sub>. By 10 days, the  $\gamma_2$  phase was totally transformed to  $\gamma_3$  phase. By 40 days, the Zn phase had precipitated near the  $\gamma_3$  phase. How-

ever, the reaction was different in the way that sub-micron (Al, Au, Zn) particles formed inside the solder ball and maintained the phase stability with Sn or Zn phase during this aging period. The (Al, Au, Zn) phase was usually found to aggregate around the band-shaped IMC (Fig. 4). This aggregation may have occurred because, in this region that was Au rich during the reflow process, Au had reacted with both Al and Zn in the liquid solder.

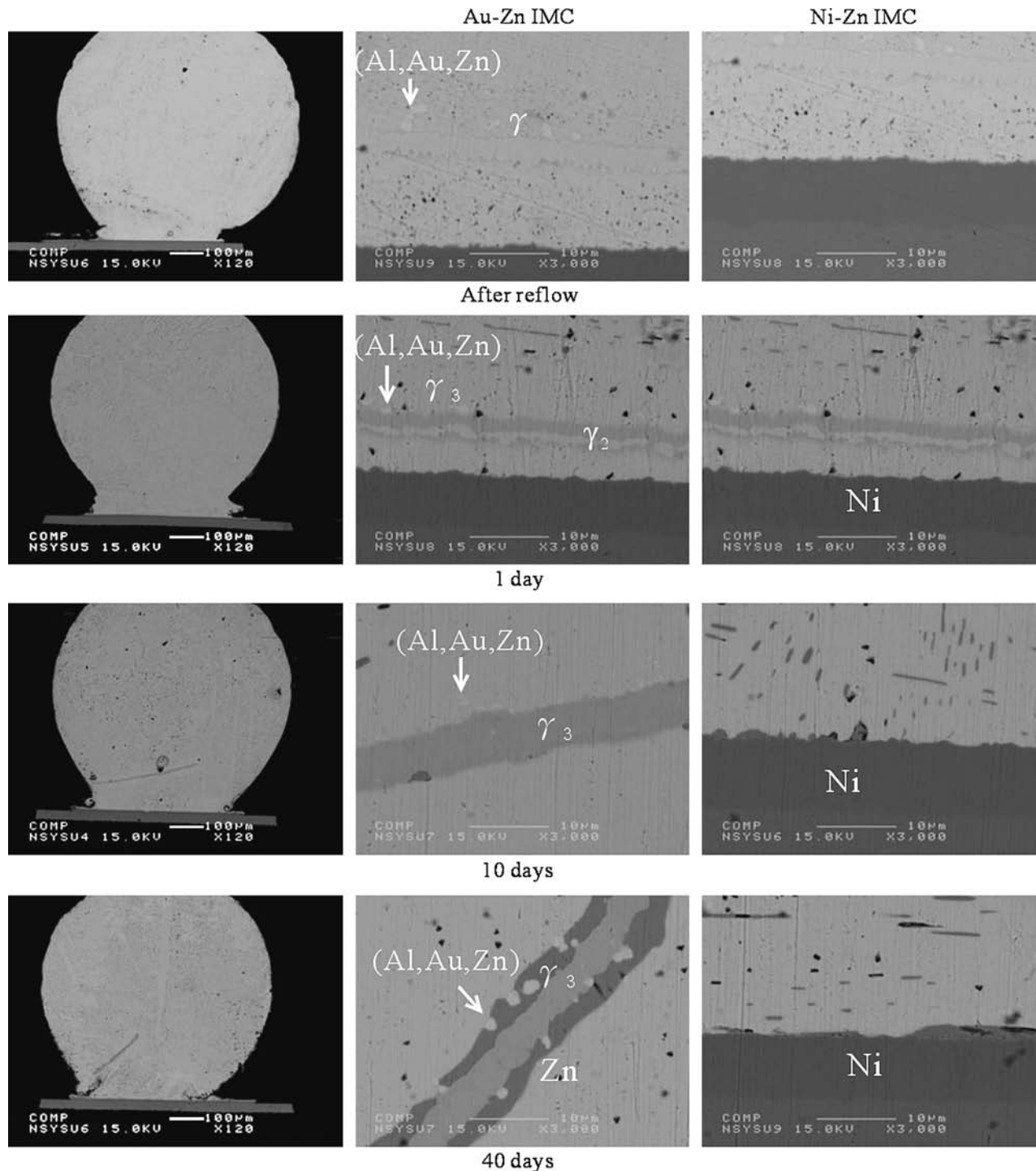


Fig. 4. SEM micrographs of Sn-Zn-Al solder balls with 150°C aging in various days.

We could not, however, precisely determine the composition of (Al, Au, Zn) particles using EPMA, because of the micron size particle that formed within the Zn phase and because the cross section planarity is poor. The total count of Al, Au, and Zn elements made up less than 95 wt.%. Our best estimation of this phase found it to be similar to  $\text{Al}_2(\text{Au}, \text{Zn})$  in composition. The reaction was also different from the reaction in Sn-9Zn solder in that no  $\text{Ni}_5\text{Zn}_{21}$  had formed in the interface after 50 days of aging. At that time, only a thin layer (Al, Au, Zn) IMC was observed to have formed above the Ni layer at the interface. Sn-9Zn solder differed significantly from Sn-Zn-Al solder in this way.

Our results showed that adding 0.01 wt.% Al did not affect the reaction of Au and Zn in the solder balls and it stopped the reaction of Ni and Zn at the interface, suggesting that this thin layer of (Al, Au, Zn) IMC may play a key role in impeding the reaction of Ni and Zn. The Al has been reported to condense easily in the interface in the Sn-Zn-Al-X solders.<sup>10-15</sup> A thin layer of  $\text{Al}_2(\text{Au}, \text{Zn})$  compound has been reported at the interface with electroless Ni-P/Au finish bond pad surface.<sup>15</sup> Figure 5 shows the fracture surface after ball shear test for a Sn-Zn-Al solder sample that had been aged 10 days in this study. The figure shows brittle fracture morphology corresponding with much lower ball shear strength. The ball shear test results for BGA256 package with Sn-Zn and Sn-Zn-Al solder ball are plotted in Fig. 6a and b with the maximum and minimum values. The ball shear test was performed on 32 selected balls on each BGA256 package that been aged over different periods of time. Sn-Zn-Al solder balls with lower ball shear test values were found to have brittle fracture surfaces. The exact composition of the intermetallic phase that had formed at the interface could not be identified because it was too thin. The 10 Kev energy-dispersive spectroscopy and wavelength dispersive spectrometer (WDS) analyses found peaks in Al, Au, and Zn, but no peaks in Ni. This phase could be  $\text{Al}_2(\text{Au}, \text{Zn})$  phase.<sup>15</sup> It has been reported that a sim-

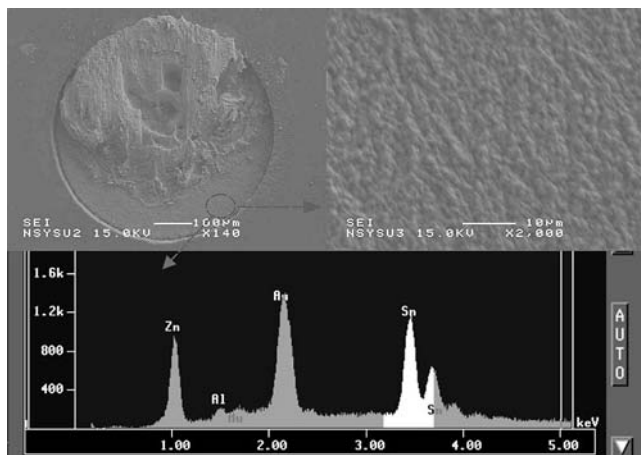


Fig. 5. The ball-shear test surface of Sn-Zn-Al solder balls under 150°C aging for 10 days. The marked flat area is (Al, Au, Zn) phase according to X-ray analysis.

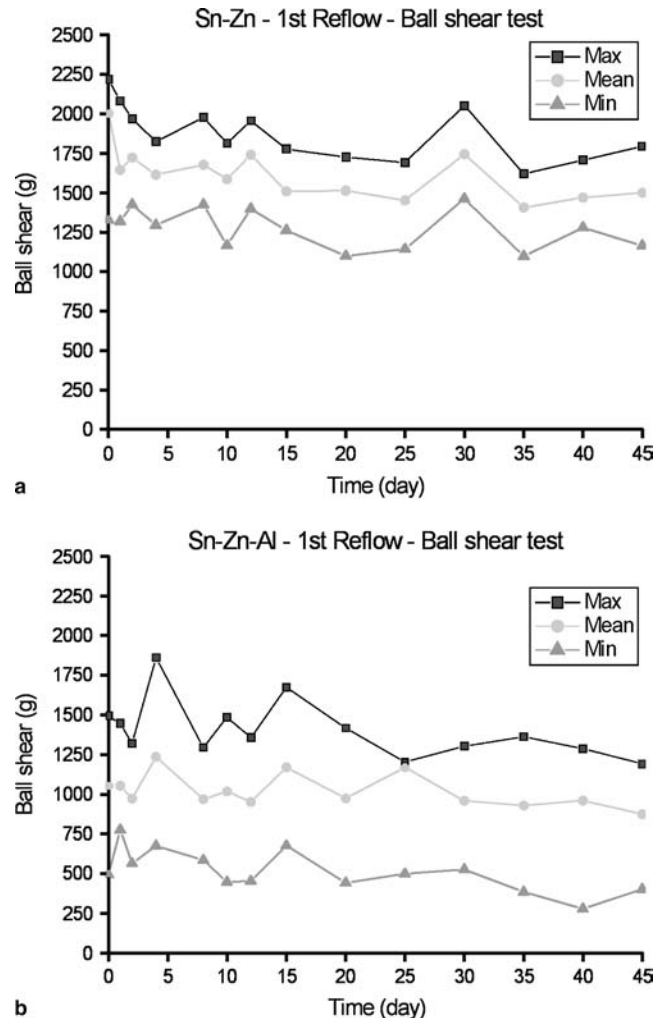


Fig. 6. (a) Ball shear test results of BGA256 with Sn-Zn solder ball. (b) Ball shear test results of BGA256 with Sn-Zn-Al solder ball.

ilar thin layer of  $\text{Al}_{4.2}\text{Cu}_{3.2}\text{Zn}_{0.7}$  compound forms at the interface of Sn-Zn-Al solders and Cu substrate.<sup>10</sup> The compound in that study provided a barrier to Sn diffusion toward Cu substrate and thus no Cu-Sn compound could be detected. The results have been the same in studies of Sn-8.55Zn-1Ag-XAl solders<sup>12</sup> and Sn-Zn-Ag-Ga-Al solders<sup>13</sup> and their reactions to Cu substrates.

Based on our results, it can be concluded that in Sn-Zn solders using Al, Al prefers to react with Au and Zn, a reaction that forms (Al, Au, Zn) particles in the solder and in thin layer (Al, Au, Zn) IMC at the interface during the reflow process. The formation of the (Al, Au, Zn) particles acted as the reaction barrier. The lower ball shear strength corresponds with brittle fracture morphology.

### Diffusion Behavior of Zn during Aging

The Zn was found to be a dominant diffusing element, inducing the formation of Au-Zn IMC and  $\text{Ni}_5\text{Zn}_{21}$ . The sequence of IMC formation is schematically described in Fig. 7. The Zn diffused into the Au-Zn IMC and  $\text{Ni}_5\text{Zn}_{21}$  at the same time during the aging of the samples at 150°C. The Au-Zn IMC

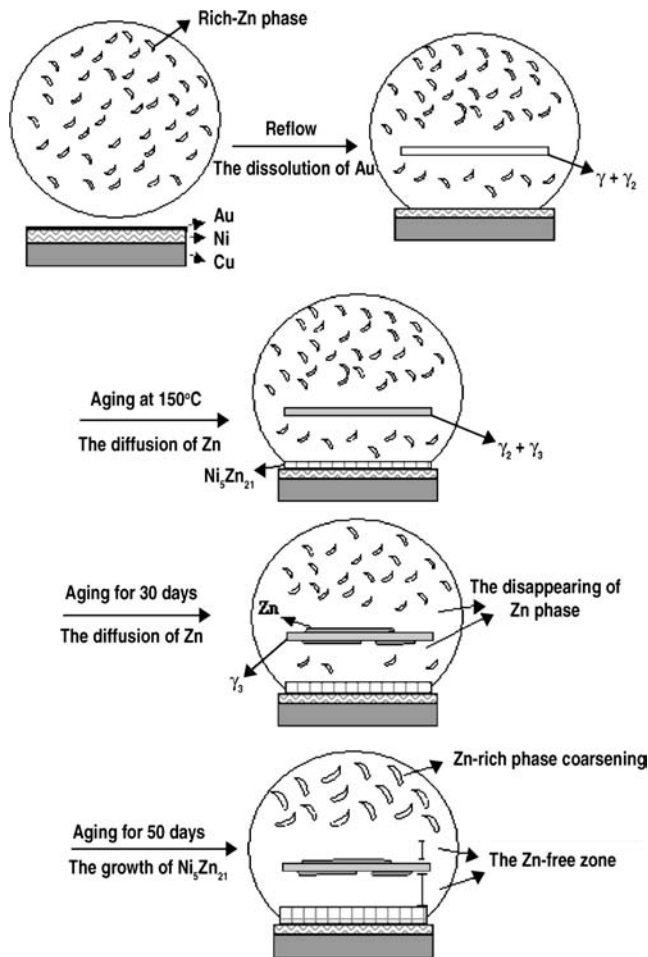


Fig. 7. The schematic Zn diffusion and IMC formation sequence diagram.

changed from  $\gamma$  plus  $\gamma_2$  phases to  $\gamma_3$  phase, the composition of the phases forwarded to enrichment of Zn. Finally, as a result of the saturation of the IMC, Zn precipitated next to the  $\gamma_3$  phase, a finding consistent with the Au-Zn binary phase diagram. Because quantities of Au were limited, Au-Zn IMC maintained its thickness during the aging period. However, with Zn diffusing into the Ni layer, the  $\text{Ni}_5\text{Zn}_{21}$  phase continuously increased in thickness during the aging period. The composition of the  $\text{Ni}_5\text{Zn}_{21}$  phase remained similar and no new phase formed in the Ni interface, suggesting that  $\text{Ni}_5\text{Zn}_{21}$  was able to remain stable under these test conditions. Because Zn was always consumed during the formation and growth of the IMCs with Au and Ni, Zn-free zones developed near these IMC regions after long periods of aging.

The Zn behaved somewhat differently when reacting with Au/Ni surface finishes in Sn-Zn-Al solder balls. A thin layer (Al, Au, Zn) IMC formed on the Ni layer and blocked the formation of  $\text{Ni}_5\text{Zn}_{21}$ . The

Zn-free zone was found only inside the solder ball around the band-shaped Au-Zn IMC.

## CONCLUSIONS

The Au dissolved into the solder balls and formed a band-shaped phase as  $\gamma\text{-Au}_3\text{Zn}_7$  and  $\gamma_2\text{-AuZn}_3$  during solder reflow. With aging,  $\gamma\text{-Au}_3\text{Zn}_7$  and  $\gamma_2\text{-AuZn}_3$  transformed into  $\gamma_3\text{-AuZn}_4$ . The interfacial reaction in the solder balls with Ni layer resulted in the formation of  $\text{Ni}_5\text{Zn}_{21}$ . Because Zn kept diffusing to form the Au-Zn IMC and  $\text{Ni}_5\text{Zn}_{21}$ , Zn-free zones developed near both IMC regions. In the Sn-Zn-Al solder balls, thin layer (Al, Au, Zn) IMC formed in the interface of the Ni layer and inhibited the formation of  $\text{Ni}_5\text{Zn}_{21}$ . Fine (Al, Au, Zn) particles formed resembling  $\text{Al}_2(\text{Au, Zn})$  in composition and remained stable in the solder. The transformation of Au-Zn IMC in the Sn-Zn-Al solder balls was similar to that in the Sn-9Zn solder balls.

## ACKNOWLEDGEMENTS

Ker-Chang Hsieh thanks the NSC for its financial support (NSC Grant No. 92-2216-E-110-016). The authors also thank the Technical Development Division of Philips at Taiwan for their preparation of the samples.

## REFERENCES

1. K. Zeng and K.N. Tu, *J. Mater. Sci. Eng. Rep.* 38, 55 (2002).
2. A. Zribi, A. Clark, L. Zavaliy, P. Borgesen, and E.J. Cotts, *J. Electron. Mater.* 30, 1157 (2001).
3. L.C. Shiau, C.E. Ho, and C.R. Kao, *Soldering Surface Mount Technol.* 14, 25 (2002).
4. M.N. Ahemd Sharif, *Mater. Sci. Eng., B* 113, 184 (2004).
5. K.S. Kim, S.H. Huh, and K. Sukanuma, *Des. Issues* 352, 226 (2003).
6. K.S. Kim, K.W. Ryu, C.H. Yu, and J.M. Kim, *Microelectron. Reliability* 45, 647 (2005).
7. K.S. Kim, J.M. Yang, C.H. Yu, I.O. Jung, and H.H. Kim, *J. Alloys Compounds* 379, 314 (2004).
8. M. Date, K.N. Tu, T. Shoji, M. Fujiyoshi, and K. Sato, *J. Mater. Res.* 19, 2887 (2004).
9. M. Date, K.N. Tu, T. Shoji, M. Fujiyoshi, and K. Sato, *Scripta Mater.*, 51, 641 (2004).
10. K.L. Lin and H.M. Hsu, *J. Electron. Mater.* 30, 1068 (2001).
11. S.P. Yu, M.C. Wang, and M.H. Hon, *J. Mater. Res.* 16, 76 (2004).
12. S.C. Cheng and K.L. Lin, *J. Electron. Mater.* 31, 940 (2002).
13. C.M. Chuang, H.T. Hung, P.C. Liu, and K.L. Lin, *J. Electron. Mater.* 33, 7 (2003).
14. C.W. Huang and K.L. Lin, *J. Mater. Res.* 19, 3560 (2004).
15. C.W. Huang and K.L. Lin, *Mater. Trans.* 45, 588 (2004).
16. T.B. Massalski, H. Okamoto, P.R. Subramanian, and L. Kacprzak, eds., *Binary Alloy Phase Diagrams* (Materials Park, OH: ASM International, 1990), pp. 456–458.
17. T.B. Massalski, H. Okamoto, P.R. Subramanian, and L. Kacprzak, eds., *Binary Alloy Phase Diagrams* (Materials Park, OH: ASM International, 1990), pp. 2887–2889.
18. Y.C. Chan, M.Y. Chiu, and T.H. Chuang, *Z. Metallkd.* 93, 95 (2002).